OCA-B/Pou2af1 is sufficient to promote CD4$^+$ T cell memory and prospectively identifies memory precursors

Wenxiang Sun[1,2,†], Erik P. Hughes[1,2,†], Heejoo Kim[1,2,†,Ψ], Jelena Perovanovic[1,2,§], Krystal R. Charley[1,2], Bryant Perkins[1], Junhong Du[1,2], Andrea Ibarra[1,2], Amber R. Syage[1,2], J. Scott Hale[1], Matthew A. Williams[1,2], Dean Tantin[1,2,3,*]

[1]Department of Pathology, University of Utah School of Medicine, Salt Lake City, UT 84112, U.S.A.
[2]Huntsman Cancer Institute, University of Utah School of Medicine, Salt Lake City, UT 84112, U.S.A.
[3]Lead contact

[*]Correspondence author: Dean Tantin
Email: dean.tantin@path.utah.edu

Author contributions:
J.S.H, M.A.W., D.T. designed research; W.S., E.P.H., H.K., K.R.C., B.P., J.D., A.I. performed research; J.S.H., M.A.W. contributed research tools; W.S., E.P.H., H.K., J.P., K.R.C., B.P., A.R.S analyzed data; W.S., E.P.H., H.K., J.P., K.R.C., J.D., A.I., J.S.H., M.A.W., D.T. wrote the manuscript.

Competing interest statement: The authors declare that they have no competing interests.
Classification: Immunology
Keywords: Immunological memory | CD4 T cells | Pou2af1/OCA-B

[†]Equal contributors
[Ψ]Current address: Janssen Research & Development, LLC., Neuroimmunology Drug Discovery, 3210 Merryfield Row, San Diego, CA 92121.
[§]Current address: Recursion Pharmaceuticals, 41 400 W, Salt Lake City, UT 84101

Words in abstract: 152
Words in MS (excluding references): 6,853

Abstract

The molecular mechanisms leading to the establishment of immunological memory are inadequately understood, limiting the development of effective vaccines and durable anti-tumor immune therapies. Here we show that ectopic OCA-B expression is sufficient to improve antiviral memory recall responses, while having minimal effects on primary effector responses. At peak viral response short lived effector T cell populations are expanded but show increased *Gadd45b* and *Socs2* expression, while memory precursor effector cells show increased expression of *Bcl2*, *Il7r* and *Tcf7* on a per-cell basis. Using an OCA-B mCherry reporter mouse line, we observe high OCA-B expression in $CD4^+$ T_{CM} cells. We show that early in viral infection, endogenously elevated OCA-B expression prospectively identifies memory precursor cells with increased survival capability and memory recall potential. Cumulatively, the results demonstrate that OCA-B is both necessary and sufficient to promote CD4 T cell memory in vivo and can be used to prospectively identify memory precursor cells.

Significance

$CD4^+$ T cell memory is incompletely defined and memory progenitors difficult to identify. Here, we show that expression of the OCA-B transcription coactivator in $CD4^+$ T cells is necessary and sufficient to drive productive memory. Using a novel mCherry reporter mouse line, we show that OCA-B expression enriches for responding effector cells with elevated memory potential. The results show that OCA-B expression in T cells is sufficient to promote $CD4^+$ memory formation and marks memory precursor cells.

53 **Introduction**

54 The ability to respond robustly to secondary antigen exposures (immune memory) is a defining
55 feature of the adaptive immune system and forms the physiologic basis for vaccination (1). Immune
56 memory can also drive autoimmune and antitumor responses (2-5). Strategies that promote memory
57 have the potential to improve both vaccine efficacy and tumor immunotherapy. Central memory T
58 cells (T_{CM}), which home to secondary lymphoid organs, are particularly long lived and demonstrate
59 high proliferative capacity upon antigen reencounter.

60 Multiple transcription factors and epigenetic regulators are known to modulate T_{CM} formation or
61 function, including Id3 (6), Blimp1 (7-9), Suv39h1 (10), T-bet (11, 12), Foxo1 (13, 14), Bcl6 (15, 16),
62 Eomes (17) and TCF1 (18). Many of these factors regulate memory more clearly in $CD8^+$ compared to
63 $CD4^+$ T cells. In $CD4^+$ T cells, the lymphocyte-restricted transcriptional coregulator OCA-B (also
64 known as OBF-1 and Pou2af1) is induced upon T cell antigen stimulation (19, 20). T cells from
65 germline OCA-B deficient mice mount normal primary T cell responses to lymphocytic
66 choriomeningitis virus (LCMV) but show attenuated $CD4^+$ memory T cell formation and recall
67 response (21). Elevated *Ocab* (*Pou2af1*) mRNA levels are seen in $CD4^+CD25^{lo}$ early effector cells
68 that are enriched for memory potential (22). OCA-B is also associated with autoimmunity (23-26).

69 Here, we show that OCA-B deletion in T cells selectively reduces $CD4^+$ T cell memory
70 potential. We show that ectopic OCA-B expression minimally affects peak $CD4^+$ T cell responses to
71 LCMV, but is sufficient to expand antigen recall responses at the expense of empty vector (EV)-
72 transduced controls. mRNA expression profiling of effector cells ectopically expressing OCA-B reveals
73 gene expression changes associated with effector and memory properties, signaling and homing.
74 These include global increases in *Socs2* and *Gadd45b*, expansion of short-lived terminal effector T
75 cell populations, and increases in *Tcf7* and *Il7r* in specific memory precursor populations. Using an
76 OCA-B reporter mouse, we show that elevated levels of endogenous OCA-B in effector T cells during
77 the primary response prospectively identifies $CD4^+$ T effector cells with enhanced survival and
78 expansion capability.

79

80 **Results and Discussion**

81 **OCA-B in T cells is required for robust $CD4^+$ T cells memory recall response**

82 We used a conditional *Ocab* (*Pou2af1*) mouse allele crossed to a CD4-Cre driver, which efficiently
83 deletes OCA-B in T cells (26), to study effects of T cell-specific OCA-B loss. We infected $Ocab^{fl/fl}$;CD4-
84 Cre and control $Ocab^{fl/fl}$ mice with $LCMV^{Arm}$ and measured specific T cell responses using $I\text{-}A^b/gp_{66-77}$
85 tetramer staining. No significant differences in the frequency of $CD4^+$ $I\text{-}A^b/gp_{66-77}{}^+$ $CD4^+$ T cells were
86 observed at 8 days post-primary infection (dpi, Fig. S1*A*-*B*, D8). Rechallenging these mice with
87 *Listeria monocytogenes* expressing the LCMV glycoprotein epitope (Lm-gp61) (27) elicited a trending
88 but nonsignificant decrease in the frequency of cells undergoing memory recall response in

89 *Ocab*$^{fl/fl}$;CD4-Cre mice (Fig. S1*A*-*B*, D40+7). The responding cells did however show a significant
90 decrease in IFNγ production (Fig. S1*C*-*D*). The same cells showed minimal changes in ICOS, PD-1,
91 Ly6C or CD62L (Fig. S1*E*). These results indicate that infection of T cell-conditional OCA-B knockout
92 mice with LCMV results in deficiencies in IFNγ expression during memory recall responses.
93 The relatively small reductions in frequencies of tetramer$^+$ CD4$^+$ T cells at recall response may
94 reflect selection for a small percentage of cells escaping OCA-B deletion. This selection can be
95 circumvented using bone marrow chimeras in which conditional deficient or control cells are competed
96 against wild-type T cells in the same mice. We generated bone marrow chimeras in which wild-type
97 donors were co-engrafted with congenically-marked *Ocab*$^{fl/fl}$;CD4-Cre or control *Ocab*$^{fl/fl}$ cells in the
98 same recipients. After 8 weeks of engraftment, recipient mice were infected with LCMV. The ratio of
99 antigen-reactive *Ocab*$^{fl/fl}$ control effector CD4$^+$ T cells to wild-type competitor was close to 1:1 at 8 dpi.
100 OCA-B deficient (*Ocab*$^{fl/fl}$;CD4-Cre) cells were slightly reduced relative to wild-type competitor (Fig.
101 S1*F*). To investigate the effects of T cell-specific OCA-B loss on memory recall responses, we
102 rechallenged mice with Lm-gp61. Following rechallenge, the control to wild-type cell ratio remained
103 close to 1:1 at both primary and memory recall response, while wild-type competitor cells were >8-fold
104 increased at the expense of OCA-B deficient cells specifically at recall (Fig. S1*F*-*G*). These findings
105 indicate that, as with T cell-conditional Oct1 deficiency and global OCA-B deficiency (21), T cell-
106 conditional OCA-B deficiency results in severe deficiencies in CD4$^+$ T cell memory recall responses.
107
108 **Ectopic OCA-B expression is sufficient to enhance CD4$^+$ T cell memory responses**
109 To study the effect of forced OCA-B expression, we primed Ly5.1$^+$/5.2$^+$ (CD45.1$^+$45.2$^+$) SMARTA TCR
110 transgenic donor mice with GP_{61-80} peptide and transduced isolated splenic CD4$^+$ T cells ex vivo with
111 a retroviral vector expressing mouse OCA-B and GFP. In parallel, Ly5.1$^+$/5.1$^+$ control SMARTA cells
112 were transduced with GFP-expressing EV. SMARTA mice express a transgenic TCR recognizing an
113 immunodominant LCMV glycoprotein ($GP_{61–80}$) CD4$^+$ epitope (28). GFP$^+$ SMARTA cells expressing
114 OCA-B and EV controls were sorted, mixed 1:1 and adoptively co-transferred into Ly5.2$^+$/5.2$^+$
115 recipients (Fig. 1*A*). Efficient OCA-B expression was confirmed in primary CD4$^+$ T cells (Fig. 1*B*). After
116 transfer, recipient mice were infected with LCMV and the cell populations were detected by flow
117 cytometry using congenic markers from the donor T cells and GFP expressed from the viral vector. At
118 8 dpi, splenic effector EV and OCA-B transduced cells expanded equivalently (Fig. 1*C* and D).
119 Another group of mice were infected with LCMV and allowed to clear the virus and form memory.
120 Recall responses were induced by re-challenge using Lm-gp61. At static memory timepoints (40 dpi)
121 slight but statistically nonsignificant skewing towards the OCA-B population was noted, however at
122 peak T cell response to rechallenge (40+7 dpi), ~50-fold more OCA-B overexpressing SMARTA cells
123 were present (Fig. 1*C*-*E* and Fig. S2*A*). Although memory recall potential was improved, increases in

124 Tbet and Granzyme B (Gzmb), and decreases in CXCR5, Bcl6 and TCF1 at 8 dpi were consistent
125 with an increased Th1 phenotype in OCA-B transduced cells (Fig. 1*F*, *G* and Fig. S2*B*). No significant
126 differences in IFNγ and Ki-67 were observed at 8 dpi (Fig. 1*H* and *I*). Additionally, IL-7R MFI was
127 significantly decreased in OCA-B expressing cells although cells with strong expression could still be
128 identified (Fig. S2*C*). The ability of ectopic OCA-B to promote memory recall responses was also
129 observed at longer timepoints in both spleen as well as peripheral blood (Fig. J and K and Fig. S2*D*).
130 These results indicate that OCA-B expression enhances the ability of $CD4^+$ T cells to induce memory
131 responses.
132 To investigate if ectopic OCA-B expression induces gene expression changes in effector cells
133 associated with improved memory recall, we profiled gene expression using splenic SMARTA T cells
134 at 8 dpi. $CD4^+$ cells were first isolated by magnetic isolation, then congenically marked GFP^+ cells
135 were further isolated by fluorescence-activated cell sorting (FACS). We identified ~600 down-
136 regulated genes and ~200 up-regulated genes (Table S1). Unsupervised hierarchical clustering
137 identified differentially expressed gene clusters (Fig. 2*A*). Down-regulated genes included *Il7r* and
138 *Bcl6*, consistent with the flow cytometry findings at this timepoint. The top up-regulated gene,
139 *Pou2af1*, encodes OCA-B, providing a quality control. Other up-regulated genes were associated with
140 effector activity (*Tbx21*, *Zeb2*), exhaustion (*Ikzf2*/*Helios*) and attenuation of T cell signaling and
141 proliferation (*Socs2*, *Gadd45b*). *Gadd45b* promotes autoimmune disease and anti-tumor immune
142 responses (29-32). Example genome tracks are shown in Fig. 2*B*. Gene ontology (GO) analysis of the
143 up-regulated genes identified terms associated with H3K9me3 regulation. Down-regulated genes by
144 contrast were strongly associated with H3K27me3 in $CD4^+$ and $CD8^+$ memory T cells (Fig. 2*C*). ChIP-
145 X Enrichment Analysis (ChEA) (33) identifies Tp53 and Smc3 as factors that also regulate the gene
146 set induced by OCA-B ectopic expression (Fig. 2*D*). p53 and SMC3 may therefore also control
147 expression of these genes or could themselves be controlled by OCA-B to regulate gene expression.
148 Sets of significant Molecular Function, Epigenomic Roadmap and ChEA GO terms are shown in Table
149 S2.
150 Effector $CD4^+$ T cell populations are heterogeneous, with memory progenitor cells comprising
151 a small proportion of the effector T cell population (12, 22, 34). In bulk RNA-seq, increased expression
152 of genes that promote memory in rare memory progenitors may therefore be obscured by decreases
153 in larger populations of terminal effectors. To test this, we performed single-cell RNA-sequencing
154 (scRNA-seq) at D8 post-LCMV infection. Uniform manifold approximation and projection (UMAP)
155 using EV-transduced cells revealed a variety of populations (Fig. 3*A*, Table S3). Clusters 1 and 4
156 were enriched for genes such as *Id3*, *Ccr7*, *Bcl2*, *Slamf6* and *Tcf7* (both clusters), *Tox* (cluster 1), and
157 *Cxcr5*, *Il7r*, *Icos* and *Cd69* (cluster 4, Table S3). These clusters likely contain memory precursor
158 effectors. Clusters 0, 2 and 6 by contrast were enriched in *Ccl5*, *Ifng* and *Tbx21*, respectively (Table

159 S3), and likely comprise more terminally differentiated effectors. Cluster 5 was enriched for genes
160 encoding histones, cyclin-dependent kinases and proliferating cell nuclear antigen (PCNA) and likely
161 represent proliferating effectors.
162 OCA-B-transduced cells clustered more uniformly with fewer clusters (Fig. 3*B*). Cluster 0
163 effector cells were marked by *Zeb2*, *Klrg1* and *Tbx21* (Table S3). Clusters 1 and 2 were also
164 associated with effector activity. OCA-B transduced cluster 3 was associated with effector/memory
165 progenitor activity similar to EV-transduced clusters 1 and 4 (Fig. 3*C*). Although there were
166 proportionately fewer of these cells compared to the EV-transduced clusters 1 and 4, multiple
167 memory-associated genes were increased on a per-cell basis. *Tcf7* was increased by >4-fold in OCA-
168 B cluster 3 relative to other clusters, but only 2-fold in EV clusters 1 and 4 (Table S3). *Slamf6* was
169 increased by >3-fold in OCA-B cluster 3, but <2.5-fold in EV clusters 1 and 4. *Bcl2* and *Il7r* were
170 similarly more strongly expressed relative to the other clusters in OCA-B- compared to EV-transduced
171 cells. Additionally, *Foxo1* was not over-represented in either memory-associated EV cluster but was
172 enriched in OCA-B cluster 3, while *Ikzf2*, which has been associated with $CD4^+$ T cell exhaustion (35),
173 was not enriched in cluster 3 but was enriched in the equivalent EV-transduced clusters (Table S3).
174 *Id3* was enriched in OCA-B-transduced cluster 3 more than EV cluster 4 but less so than in EV cluster
175 1. These findings suggest that OCA-B transduced cells in cluster 3 are qualitatively superior to their
176 EV-transduced counterparts at forming memory. Simultaneously, OCA-B-transduced clusters showed
177 broad increases in the expression of *Socs2*, which encodes an attenuator of T cell signaling, and
178 *Gadd45b*, which promotes growth arrest (Fig. 3*C*). These changes likely attenuate effector function
179 and/or may enable a broader transition of effectors to memory progenitors.
180 Clustering EV- and OCA-B-transduced cells together allows the relative proportions of cells
181 with common gene expression features to be determined. Again, specific clusters were enriched for
182 terminal effectors (Fig. 3*D*, clusters 0, 1, 2, 4, 6), proliferating effectors (cluster 5) and effector cells
183 with memory progenitor potential (cluster 3). Feature plots for genes associated with effector cells
184 (*Tbx21*) and memory function (*Bcl6*) are shown in Fig. 3*E*. Additional plots for other genes associated
185 with memory are shown in Fig. 3*F*. In the OCA-B-transduced condition, cluster 3 contained
186 proportionately fewer cells but showed elevated expression of genes such as *Il7r* and *Gadd45b* on a
187 per-cell basis (Fig. 3*G*). These findings identify changes in gene expression in effector T cell
188 populations consistent with increased memory potential.
189
190 **OCA-B knock-in reporter mice label $CD4^+$ memory T cell populations**
191 To monitor OCA-B expression in viable cells, we knocked 3 mCherry reporter cassettes preceded by
192 P2A elements into the mouse *Pou2af1* (*Ocab*) locus. The resulting reporter allele contained the
193 mCherry cassettes inserted immediately before the stop codon and the 3' UTR (Fig. 4*A*). A successful
194 hemizygous knock-in founder and a homozygote generated by intercrossing the progeny were

confirmed by PCR (Fig. S3*A*). Hemizygous and homozygous reporter mice retained normal OCA-B protein expression (Fig. S3*B*). OCA-B was readily detectable in peripheral blood B cells from hemizygous and homozygous reporter mice (Fig. S3*C*, *D*). Peripheral T cell expression was weaker, forming a shoulder in hemizygous reporters, but an observable peak in homozygotes (Fig. S3*C*, *D*). We therefore used heterozygous mice to perform baseline characterization of B cell populations, and homozygotes to study T cells.

Robust mCherry expression could be detected in the bone marrow, peritoneal cavity, spleen and lymph nodes of specific pathogen-free hemizygous reporter mice. Total thymocytes by contrast expressed little OCA-B (Fig. S3*E*). OCA-B expression was readily detected in developing, immature and recirculating B cell populations (Fig. S3*F*). Expression was nearly uniform in the different populations, except for a small population of immature B cells that lacked OCA-B expression. Peritoneal B-1 and B-2 B cells were also homogeneous, with stronger expression in B-1 relative to B-2 cells (Fig. S3*G*). Splenic B cells can be partitioned into transitional and mature populations. T1/2/3 subsets uniformly expressed OCA-B (Fig. S3*H*). Marginal zone (MZ), follicular and non-follicular populations all expressed OCA-B strongly (Fig. S3*I*). Expression was largely uniform, but there was a significant population of newly formed $CD21^{lo}CD23^{lo}$ B cells expressing no OCA-B. The nature and significance of these cells is unknown. These results document strong reporter activity in B cell populations, with the highest level of activity in MZ and B-1 B cells. MZ B cells are largely absent in OCA-B knockout mice (36). These results indicate that the OCA-B reporter robustly labels B cells.

Gating out B cells, approximately 5% of thymocytes from unchallenged, specific pathogen-free homozygous reporter mice expressed OCA-B (Fig. S3*J*). mCherry expression could be identified in CD4/CD8 double-negative (DN), DP and SP compartments, with the highest amounts in DN and CD8 SP cells (Fig. S3*K*). In the spleen, the relative abundance of $CD4^+$ and $CD8^+$ T cells was unaltered by the reporter allele (Fig. 4*B*). Splenic $CD4^+$ T cells express mCherry at ~50-fold lower levels compared to B cells and with a wider range of expression (Fig. 4*C*). Peripheral blood T cell mCherry levels varied over a similar range (Fig. S3*C* and not shown).

We used CD62L and CD44 to stratify resting splenic $CD4^+$ and $CD8^+$ cells into naïve, activated/effector and central memory compartments. Reporter activity could be detected in approximately 7% of naïve ($CD62L^{hi}CD44^{lo}$) cells (Fig. 4*D*). The nature of these cells is unknown. Progressively larger fractions of early activated ($CD62L^{lo}CD44^{lo}$), activated ($CD62L^{lo}CD44^{hi}$) and T_{CM} ($CD62L^{hi}CD44^{hi}$) cells expressed mCherry (Fig. 4*D*). Naïve $CD8^+$ T cells showed comparatively higher expression levels, but decreased expression in the activated state and similar expression in T_{CM} cells (Fig. 4*E*). Therefore, within the $CD4^+$ T cell compartment, increased OCA-B expression as measured by mCherry fluorescence progressively labels greater fractions of naïve, activated and central memory $CD4^+$ cells.

231 **Elevated OCA-B expression prospectively enriches memory precursor CD4$^+$ T cells**
232 To assess OCA-B responses during infection, memory formation and rechallenge, we infected
233 reporter mice with LCMV and used MHC tetramers to identify splenic T cells recognizing
234 immunodominant LCMV epitopes. Prior to infection, >90% of cells were CD44^{lo} naïve phenotype. Up
235 to 30% of cells became CD44^{hi} following infection or rechallenge, and a significant number of these
236 were Tet$^+$ as expected (Fig. S4*A*, upper plots). A high fraction of activated CD44^{hi} cells expressed
237 mCherry regardless of tetramer status (Fig. S4*A*, lower plots). mCherry was gated relative to a
238 nonreporter control (Fig. S4*B*). Fewer activated CD8$^+$ cells expressed mCherry relative to nonreporter
239 controls (Fig. S4*C*,*D*). After LCMV clearance, memory timepoint CD4$^+$ cells maintained high mCherry
240 percentages (Fig. S4*A*, D43, 61.6%), though with ~2-fold lower expression per cell (Fig. S4*E*).
241 Rechallenge with Lm-gp61 to generate CD4$^+$ T cell antigen-specific recall responses reduced the
242 percentage of mCherry$^+$ cells compared to resting memory, with high-affinity tetramer$^+$ cells declining
243 from >60% to <10% mCherry (Fig. S4*A*, D42+7). In contrast, a higher percentage of CD8$^+$ reporter T
244 cells expressed mCherry prior to infection. Higher percentages of tetramer$^+$mCherry$^+$ cells were also
245 present at 5 dpi, but by 8 dpi (peak T cell response) the mCherry percentage was reduced (Fig. S4*B*).
246 Antigen specific memory CD8$^+$ T cells also showed reduced mCherry levels relative to CD4$^+$ (Fig.
247 S4*B*). We did not collect data for CD8$^+$ rechallenge because Lm-gp61 does not express the CD8-
248 dominant epitope recognized by H2-D^b LCMV tetramers.
249 To determine if OCA-B expression in responding CD4$^+$ T cells is associated with increased
250 memory potential, we crossed the reporter allele to a SMARTA TCR transgenic background to fix the
251 TCR specificity and to Ly5.1 to track engrafted cells. We transferred cells into recipients, infected with
252 LCMV, isolated mCherry^{hi} and mCherry^{lo} cells at 8 dpi, transferred large numbers of cells (8×10^5) into
253 naïve secondary recipient mice, and isolated splenic CD4$^+$ T cells to assess contraction (Fig. 5*A*).
254 mCherry gating for the cells is shown in Fig. S4*F*. More cells were recovered from mice engrafted with
255 mCherry^{hi} cells, indicating that these cells contracted less than mCherry^{lo} controls (Fig. 5*B*, *C*).
256 Interestingly the cells that did survive showed similar mCherry levels (Fig. 5*D*). These findings indicate
257 that effector CD4$^+$ cells expressing higher OCA-B contract less when transferred into naïve animals.
258 To test the ability of OCA-B expressing cells to mount antigen recall responses, we similarly
259 transferred congenically marked SMARTA cells into recipient mice and infected with LCMV, but
260 collected mCherry^{hi} and mCherry^{lo} cells at 43 dpi. 4×10^4 memory SMARTA cells were transferred into
261 naïve hosts, which were challenged with LCMV and analyzed at 7 dpi (Fig. 5*E*). mCherry^{hi} SMARTA
262 cells responded better compared to mCherry^{lo} (Fig. 5*F*, *G*) though again with expression normalizing
263 following antigen re-encounter (Fig. 5*H*). Example flow cytometry plots are shown in Fig. S4G.
264 In mice, OCA-B expression can be detected, varying over a 10-fold range, in responding cells
265 as early as one day after LCMV infection (21). Memory progenitor cells characterized by low CD25

266 expression can be identified as early as early as 3 dpi (15, 22). We transferred SMARTA homozygous
267 OCA-B mCherry reporter T cells into congenic recipients, infected with LCMV, and collected spleens
268 at 3 dpi to study mCherry and CD25 levels (Fig. 5*I*). A large fraction of responding $CD25^{lo}$ SMARTA
269 cells expressed mCherry (Fig. 5*J*). SMARTA cells from the same mouse expressing low levels of
270 CD25 also expressed high levels of TCF1, as expected (22). mCherry and TCF1 were not compared
271 as cell fixation quenches mCherry, however we were able to directly compare CD25 and OCA-B.
272 $CD25^{hi}$ cells expressed a range of OCA-B, while $CD25^{lo}$ cells were highly enriched for $mCherry^{hi}$ cells
273 (Fig. 5*K*, *L*). These findings show that high OCA-B expression can be used to prospectively mark live
274 $CD4^{+}$ memory precursor effector T cells with augmented capacity to form central memory.
275 Cumulatively, this study indicates that OCA-B expression within $CD4^{+}$ T cells is both necessary for,
276 and sufficient to promote, the emergence of T_{CM}.

277 **Materials and methods**

278 **Mice**

279 All mice used in this study were on the C57BL6/J strain background. All mouse experiments were
280 approved by the University of Utah Institutional Animal Care and Use Committee (protocol 00001553).
281 *Pou2af1* (*Ocab*) conditional (floxed) mice were described previously (26). *Pou2af1*-3×mCherry
282 reporter knock-in mice were generated on a C57BL/6N background (Biocytogen), but were
283 backcrossed >5 times to C57BL/6J prior to generation of data herein.

284

285 **LCMV and *Listeria* infection**

286 LCMV Armstrong 53b ($LCMV^{Arm}$) (37) was grown in BHK cells and titered using Vero cells (28). For
287 primary infection, 8-to 12-week-old $Ocab^{fl/fl}$ or $Ocab^{fl/fl}$;CD4-Cre mice were inoculated i.p. with 2×10^5
288 plaque-forming units (PFU) of LCMV intraperitoneally.
289 For heterologous rechallenge with *Listeria monocytogenes* expressing LCMV glycoprotein 61-80 (Lm-
290 gp61) (27), bacteria were grown in log phase in BHI media, and concentrations were calculated using
291 OD at 600 nm (OD of $1=1\times10^9$ CFU/mL). Mice were rechallenged intravenously (i.v.) with 2×10^5
292 colony forming units (CFU) of Lm-gp61 the indicated number of days after primary infection as
293 published (38).

294

295 **Bone marrow radiation chimeras**

296 Radiation chimeras were generated as published (39). Briefly, male Ly5.1 C57BL/6J mice were used
297 as recipients. Mice received a split dose of 900 Rad (2×450 RAD, spaced 1 hr apart), and were
298 engrafted one day later with 1 million mixed donor bone marrow cells. Competitor bone marrow cells
299 from Ly5.2/Thy1.1 but otherwise wild-type mice, and experimental cells from Ly5.2/Thy1.2 $Ocab^{fl/fl}$ or
300 littermate $Ocab^{fl/fl}$;CD4-Cre mice, were isolated from femurs and tibias of donor mice. After red blood
301 cell lysis, $CD3^+$ cells were depleted using biotinylated anti-CD3 antibodies (eBioScience) and anti-
302 biotin magnetic MicroBeads (Miltentyi Biotech) according to the manufacturer's instructions. CD3-
303 depeleted bone marrow cells were mixed 1:1 and injected retro-orbitally. The chimeras were rested
304 for 8 weeks to allow engraftment, after which mice were infected as above. Virus-reactive cells were
305 identified by $LCMVgp_{66–77}$:I-Ab tetramer staining.

306

307 **pMSCV-IRES-GFP-OCA-B vector generation**

308 Wild-type *Ocab* cDNA was amplified from the plasmid pcDNA3.1-OCA-B (40) (a gift from Robert
309 Roeder, Rockefeller University) by PCR and cloned into the pMSCV-IRES-GFP (pMIGR1) retroviral
310 vector (a gift from Ryan O'Connell, University of Utah). Primers used for amplification were mOcab-F-
311 XhoI, 5'CTCGAGCTGTCTGCTTCAAAGAGAAAAGGCAAC; mOcab-R-*Eco*RI, 5'

312 GAATTCCTAAAAGCCCTCCACGGAGAGGGT. The PCR product was gel purified, digested with
313 *Eco*RI and *Xho*I, and inserted into a similarly digested pMIGR1 backbone using T4 DNA ligase to
314 generate pMIGR1-OCA-B. All constructs were validated by resequencing.
315
316 **CD4$^+$ T cell isolation and stimulation**
317 Naïve splenic CD4$^+$ T cells were isolated and simulated as described previously (41). Briefly, spleens
318 were dissociated by grinding and passing through a 70 μm nylon strainer. Red blood cells were lysed
319 by ACK lysis buffer (150 mM NH_4Cl, 10 mM $KHCO_3$, 0.1 mM EDTA). Cells were isolated from mice
320 using a naïve CD4$^+$ T cell isolation kit (Miltenyi), and stimulated in culture using 10 μg/mL plate-bound
321 anti-CD3ϵ and 2 μg/mL anti-CD28 antibodies (eBioscience).
322
323 **Ectopic OCA-B expression in CD4$^+$ T cells**
324 Ly5.1$^+$/5.1$^+$ SMARTA and Ly5.1$^+$/5.2$^+$ SMARTA donor mice were i.v. primed with 200 μg GP_{61-80}
325 peptide (AnaSpec). The next day, T cells were purified using a CD4$^+$ T cell isolation kit (Miltenyi).
326 Cells were transduced by spin infection with pMIGR retroviruses packaged in 239T cells, with or
327 without mouse OCA-B cDNA. For spin infection, cells were centrifuged with 293T retroviral
328 supernatant at 1000×*g* for 2 hr at 37°C in the presence of 4 μg/mL polybrene (Sigma). Following spin
329 infection, cells were cultured in RPMI 1640 medium supplemented with 10% fetal bovine serum, 50
330 U/mL penicillin, 50 μg/mL streptomycin, 2 mM L-glutamine, 1 mM sodium pyruvate, 1× MEM
331 nonessential amino acids, 55 μM 2-mercaptoethanol, and 20 IU/mL recombinant human IL-2 for two
332 days. All components were from ThermoFisher with the exception of IL-2, which was supplied by R&D
333 Systems. After two days, transduced GFP$^+$ cells were isolated by FACS (BD FACSAria). 1×10^4
334 pMIGR1- and pMIGR1-OCA-B-transduced cells were combined and co-transferred into wild-type
335 (Ly5.2/5.2) C57BL6/J mice. Chimeric mice were infected with LCMV and re-challenged with Lm-gp61
336 as described above. For the experiment shown in Fig. 1*J*, *K*, T cells from Ly5.1 SMARTA and Thy1.1
337 SMARTA mice were purified using a CD4$^+$ T cell isolation kit (Miltenyi) and stimulated with
338 CD3ϵ/CD28 for 2 days followed by spin transfection.
339
340 **Flow cytometry**
341 Spleens were dissociated and passed through a 70 μm nylon strainer. Red blood cells were lysed by
342 ACK lysis buffer (150 mM NH_4Cl, 10 mM $KHCO_3$, 0.1 mM EDTA). For intracellular staining, cell
343 suspensions in RPMI supplemented with 10% fetal bovine serum were re-stimulated for 4 hr with 1
344 μM LCMV $GP_{61–80}$ or 0.1 μM GP_{33-41} peptide along with Brefeldin A (GolgiPlug Becton-Dickinson, 1
345 μl/mL) as published (42, 43). Cells were subsequently fixed by cell fixation/permeabilization solution
346 (Cytofix/Cytoperm, Becton-Dickinson) according to the manufacturer's protocol. For tetramer staining,

347 APC-conjugated $gp_{66–77}$:I-A^b and gp_{33-41}:H-$2D^b$ tetramers were provided by the NIH Tetramer Core
348 Facility (Emory Vaccine Center). Cell suspensions were incubated at 37°C for 3 hr in RPMI with the
349 tetramer followed by cell-surface staining. Tetramer fluorescence was normalized with isotype
350 tetramer (hCLIP:I-A^b) staining. Fig. 1*C, H*, and *I* were generated using a Cytek Aurora spectral
351 cytometer. All other flow cytometry data were generated using a BD Fortessa LSR. The following anti-
352 mouse antibodies were supplied by Ebioscience: CD4-APC (RM4-5), CD3-Biotin (145-2C11),
353 CD90.2-FITC (53-2.1), IL-2-PE (JES6-5H4), IFNy-APC (XMG1.2), CD8a-PerCP/Cy5.5 (53-6.7),
354 CD90.1/Thy1.1-APC (HIS51). The following antibodies were supplied by Biolegend: CD4-
355 PerCP/Cy5.5 (RM4-5), CD44-APC/Cy7 (IM7), CD278/ICOS-BV510 (C398.4A), CD62L-FITC (MEL-
356 14), CD279/PD-1-BV605 (29F.1A12), CD45.1-PerCP-Cy5.5 (A20), CD45.1-BV711 (104), CD45.2-
357 FITC (104), IgM-APC/Cy7 (RMM-1), B220-APC (RA3-6B2), CD21-PE (7E9), CD23-FITC (B3B4),
358 CD93-APC (AA4.1), CD19-FITC (1D3/CD19), Tbet-APC (4B10), CXCR5-PE-Cy7 (L138D7),
359 CD127/IL7Ra-PE/Cy5 (A7R34), IFNy-APC (XMG1.2), CD8a-APC (53-6.7). The following antibodies
360 were supplied by BD Biosciences: Ly-6C-BV450 (AL-21), Bcl6-BV421 (k112-91), Tcf1-PE (S33-966),
361 Ki67-V450 (B56), CD4-BUV395 (GK1.5), CD19-BUV661 (ID3), CD8a-BUV737 (53-6.7). Gzmb-PE
362 (NGZB) was supplied by Invitrogen. Tcf1-AF488 (C63D9) was supplied by Cell Signaling.

363

364 **Bulk RNAseq**

365 $CD4^+$ T cells were purified from female Ly5.1 SMARTA and Ly5.1/5.2 SMARTA mice, and separately
366 transduced with pMIGR1-OCA-B or pMIGR1 (EV), respectively. On the following day, transduced
367 GFP^+ cells were sorted, 20,000 of each combined 1:1, and injected intravenously into 24 male
368 C57BL/6J male recipients. 24h later, each recipient mouse was injected intraperitoneally with $2x10^5$
369 pfu LCMV. After eight days, the 24 mice were divided into six groups of four mice by combining four
370 spleens together. $CD4^+$ T cells were purified using a Miltenyi CD4 T cell isolation kit. Cells then were
371 stained with PerCP-Cy5.5 Ly5.1 and AF700 Ly5.2 antibodies. $GFP^+Ly5.1^+Ly5.2^+$ (EV) and
372 $GFP^+Ly5.1^+$ (OCA-B-expressing) cells were sorted by FACS and used for RNA purification (RNeasy
373 Mini Kit, QIAGEN). RNA concentrations were determined using a Quant-iT RNA assay kit and a Qubit
374 fluorometer (ThermoFisher). Because limited RNA from EV-transduced cells was obtained, the six EV
375 samples were combined into three samples. Five OCA-B-transduced samples (each comprising four
376 mice) were submitted for RNAseq analysis. These showed a high degree of concordance (not
377 shown). Total RNA samples (200-500 ng) were hybridized with Ribo-Zero Plus (Illumina) to deplete
378 cytoplasmic and mitochondrial and ribosomal RNA from samples. RNA sequencing libraries were
379 prepared as described using the Stranded Total RNA Prep, Ligation with Ribo-Zero Plus kit (Illumina)
380 and IDT for Illumina RNA UD Indexes Set A, Ligation (Illumina). Purified libraries were qualified on an
381 Agilent Technologies 2200 TapeStation using a D1000 ScreenTape assay. The molarity of adapter-

382 modified molecules was defined by qPCR using the Kapa Biosystems Kapa Library Quant Kit.
383 Individual libraries were normalized to 0.65 nM in preparation for Illumina sequence analysis.
384 Sequencing libraries were chemically denatured and applied to an Illumina NovaSeq flow cell using
385 the NovaSeq XP workflow (20043131). Following transfer of the flow cell to an Illumina NovaSeq 6000
386 instrument, a 150 x 150 cycle paired-end sequence run was performed using a NovaSeq 6000 S4
387 reagent Kit v1.5 (Illlumina).
388
389 **Bulk RNA-seq analysis**
390 Bulk RNA-seq analysis was performed as previously described (44). Briefly, Reads were aligned to
391 *Mm10* using STAR (v2.7.3a) and checked for quality using multiqc (v1.10). Between 12 and 14 million
392 pair-end reads were generated for each sample, with >98% of aligned reads mapping to the correct
393 strand and >93% of the reads uniquely aligned to the gene. Differentially expressed genes were
394 identified using DESeq2 version 1.24.0 (45) with a 5% FDR cutoff. Features with zero counts and 5 or
395 fewer reads in every sample were removed from the analysis. Genes increased by 1.4-fold or more or
396 decreased by 2-fold or more, and with adjusted $p<0.05$ were selected as differentially expressed ($0.5 < \log2FC < -1$; padj ≤ 0.05). Figures were generated in R version 4.0.0 using functions from ggplots
398 libraries and pheatmap.
399
400 **Single-cell RNA-seq**
401 To profile gene expression at the single-cell level, splenic $GFP^+Ly5.1^+Ly5.2^+$ (EV-transduced) and
402 $GFP^+Ly5.1^+$ (OCA-B-transduced) SMARTA cells from four pooled mice per condition were isolated,
403 resuspended in PBS with 0.04% bovine serum albumin (ThermoFisher), and filtered through 40 μm
404 strainers. Viability and cell count were assessed using a Countess II (ThermoFisher). Equilibrium to
405 targeted cell recovery of 6,000 cells along with Gel Beads and reverse transcription reagents were
406 loaded to Chromium Single Cell A to form Gel-bead-in Emulsions (GEMs). Within individual GEMs,
407 cDNA generated from captured and barcoded mRNA was synthesized by reverse transcription at
408 53°C for 45 min. Samples were then heated to 85°C for 5 min. Single cell transcriptomes were
409 assessed using a 10X Genomics Chromium Single Cell Gene Expression instrument. Individual cells
410 were tagged with 16 bp barcodes, and specific transcripts with 10 bp Unique Molecular Identifiers
411 (UMIs) according to manufacturer instructions.
412
413 **Single-cell RNA-seq analysis**
414 Single cell transcriptome data were analyzed and clustered as described previously (44). Sequences
415 from the Chromium platform were de-multiplexed and aligned using CellRanger ver. 3.1.0 (10X
416 Genomics) with default parameters mm10-3.0.0. Clustering, filtering, variable gene selection and

417 dimensionality reduction were performed using Seurat ver.4.0.4 (46) according to the following
418 workflow: 1, Cells with <200 detected genes were excluded further analysis. 2, Cells with <5% UMIs
419 mapping to mitochondrial genes and *Cd44* expression >0 were retained for downstream analysis, as
420 SMARTA cells are uniformly responding to LCMV glycoprotein antigen at this time. 3, The UMI counts
421 per ten thousand were log-normalized for each cell using the natural logarithm. 4, Variable genes
422 (2000 features) were selected using the FindVariableFeatures function. 5, Common anchors between
423 the conditions were identified using FindIntegrationAnchors function that were further used to
424 integrate these sets. 6, Gene expression levels in the integrated set were scaled along each gene and
425 linear dimensional reduction was performed. The number of principal components was decided
426 through the assessment of statistical plots (JackStrawPlot and ElbowPlot). 7, Cells were clustered
427 using a shared nearest neighbor (SNN) modularity optimization-based clustering algorithm and
428 visualized using two-dimensional uniform manifold approximation and projection (UMAP). 8, One
429 cluster in each condition marked predominantly by mitochondrial genes (indicative of dying cells) was
430 excluded from the analysis. This resulted in 12,886 EV-transduced cells with 45,748 mean reads per
431 cell, and 2,595 median genes per cell. The total number of reads was 589,513,069, with 59.6%
432 mapping to exonic regions. Similarly, there were 11,709 OCA-B-transduced cells with 68,931 mean
433 reads per cell, and 2,668 median genes per cell. Total number of reads was 807,111,486, with 57.4%
434 mapping to exonic regions. Clusters were identified using manual interrogation of gene expression
435 enrichment for each population (Table S3), the ImmGene cluster identity predictor (Table S4, S5), and
436 PanglaoDB annotation terms. Clusters comprised of contaminating macrophages and neutrophils
437 were manually deleted from the visualization.
438
439 **Memory progenitor isolation, normalization and transfer**
440 To assess contraction of the effector cells with different OCA-B levels, splenic $CD4^+$ T cells were
441 purified from 8 week-old female Ly5.1/5.2 homozygous knock-in reporter, SMARTA TCR transgenic
442 mice. 2×10^4 SMARTA cells were intravenously injected into 15 male Ly5.2/5.2 C57BL/6J recipients,
443 which were infected intraperitoneally 1 day later with 2×10^5 plaque-forming units of LCMV in 250 μL
444 phosphate-buffered saline. After 8 days, responding $Ly5.1^+5.2^+$ SMARTA T cells were sorted into
445 $mCherry^{hi}$ and $mCherry^{lo}$ populations. Cells were pooled and 8×10^5 $mCherry^{hi}$ and $mCherry^{lo}$ cells
446 were separately injected intravenously into 7 naïve age-matched 9 week-old male C57BL/6J
447 secondary recipients in the case of $mCherry^{lo}$ and 5 secondary recipients in the case of $mCherry^{hi}$.
448 After 8 additional days, mice were sacrificed and splenic $Ly5.1^+5.2^+$ SMARTA cells were counted by
449 flow cytometry. To assess proliferative responses to rechallenge, 15 similar virus-naïve secondary
450 recipients were rested for 43 days post-infection prior to isolation of $mCherry^{hi}$ and $mCherry^{lo}$
451 populations. 1.3×10^4 SMARTA cells were transferred into naïve recipients, which were infected with

452 LCMV one day later. 7 days post-infection, splenic $CD4^+Ly5.1^+5.2^+$ SMARTA cells were evaluated by
453 flow cytometry. Mice with poor infection/response (total splenocyte count $<6\times10^7$) were excluded from
454 the analysis.
455
456 **Quantification and statistical analysis**
457 Excel (Microsoft) and Prism (GraphPad) were used for statistics and graphing. Two-tailed Student T-
458 tests were used to ascribe statistical significance unless otherwise indicated. For all figures, *=*p*-
459 value≤0.05; **=*p*≤0.005; ***=p<0.001. All error bars denote ± standard error of the mean.

460 **Acknowledgements:** We thank M. Chandrasekharan for help with graphics. We thank J. Marvin and
461 the University of Utah Health Sciences Center Flow Cytometry Core facility. We thank O. Allen, B.
462 Dalley and the High-Throughput Genomics Core. MHC tetramers were provided by the NIH Tetramer
463 Core Facility (Atlanta, GA). We thank R. Roeder for the mouse OCA-B cDNA and R. M. O'Connell for
464 the pMIGR1 plasmid.
465
466 **Funding:** This work was supported by NIH grants R01AI100873 and R01AI162929 to DT.
467
468
469
470 **Data and materials availability:** All data are available in the main text or the supplementary
471 materials. Materials used in the study are available to any researcher for purposes of reproducing or
472 extending the findings. Bulk and single-cell RNA-seq data have been deposited at the Gene
473 Expression Omnibus GEO) website (https://www.ncbi.nlm.nih.gov/geo/, GSE214310).

Figure legends

Fig. 1. Ectopic OCA-B expression enhances CD4+ T cell memory recall responses in vivo. (*A*) Experimental schematic for OCA-B transduction and T cell mixed adoptive transfer. Ly5.1$^+$ SMARTA cells were transduced with pMSCV-IRES-GFP (pMIGR1, EV) and Ly5.1$^+$/5.2$^+$ SMARTA cells were transduced with pMIGR1 expressing mouse OCA-B (pMIGR1-OCA-B). The donors were age- and sex-matched littermates. Two days following transduction, GFP$^+$Ly5.1$^+$ SMARTA cells (EV) and GFP$^+$Ly5.1$^+$/5.2$^+$ SMARTA cells (OCA-B) were sorted, combined 1:1, co-transferred into Ly5.2$^+$/5.2$^+$ C57BL6/J recipient mice, and infected with LCMV. Recipients were tested for static memory on day 40 post-infection, and also rechallenged with Lm-gp61 on day 40 analyzed after 7 days. (*B*) Lysates from primary CD4+ T cells transduced with either empty pMIGR1 (EV) or pMIGR1-OCA-B were immunoblotted using antibodies against OCA-B. Histone H3 is shown as an internal loading standard. (*C*) Flow cytometric analysis of Ly5.1$^+$ pMIGR1 EV-transduced and Ly5.1$^+$/5.2$^+$ pMIGR1-OCA-B-transduced (OCA-B) SMARTA cells in the spleen and blood of a representative recipient mouse at peak effector response (D8), resting memory (D40) and memory recall (D40+7). Live cells were gated based on CD4 and GFP positivity. (*D*) Ratio of OCA-B/EV transduced cells at D8, D40, and D40+7. (*E*) GFP+ cell counts per spleen for EV and OCAB transduced cells D40 and D40+7 after LCMV infection. (*F*) D8 response representative flow cytometry plots showing Tbet, Gzmb, Bcl6, Tcf1, and CXCR5 expression in splenic GFP+ CD4+ T cells by EV or OCA-B transduction condition. (*G*) Mean relative percentages of CXCR5$^-$Tbet$^+$, CXCR5$^-$Gzmb$^+$, CXCR5$^+$Bcl6$^+$, and CXCR5$^+$Tcf1$^+$ cells between transduction condition at peak response. Individual mice are connected by lines. (*H*) Representative flow plots and frequency quantification of IFNγ producing GFP$^+$ EV or OCA-B transduced cells. (*I*) Representative flow plots and frequency quantification of Ki67 producing GFP$^+$ EV or OCA-B transduced cells. (J) Representative plots showing relative percentages of splenic EV- or pMIGR1-OCA-B-transduced (GFP$^+$) SMARTA cells were plotted at D8, D52+7 and 110+7. Each datapoint represents an individual mouse harboring both EV- and pMIGR1-OCA-B-transduced cells. 5, 7 and 10 mice were sacrificed at each timepoint to obtain measurements from spleen. (*K*) Mean ratios of pMIGR1-OCA-B-transduced relative to EV-transduced SMARTA cells (OCA-B/EV) are plotted. Splenic SMARTA T cells are shown at day 8 post-infection, or 7 days post-rechallenge with Lm-gp61 (52+7 or 110+7).

Fig. 2. Gene expression changes associated with ectopic OCA-B expression in SMARTA transgenic primary effector T cells. (*A*) Heatmap showing top up- and down-regulated genes. Genes with log2 fold-change >0.5 or <-1.0, and padj $\leq$ 0.05 are shown. Example genes are shown at right. Control and OCA-B-transduced cells were purified from the same mice using magnetic isolation and FACS. (*B*) Example genome tracks showing two up-regulated genes, *Socs2* and *Gadd45b*. *Pou2af1* (*Ocab*)

509 is shown as a positive control. (*C*) Top Epigenomic roadmap and Molecular function GO terms for the
510 set of OCA-B up- and down-regulated genes. (*D*) Top ChIP-X Enrichment Analysis (ChEA 2016)
511 factors potentially regulating the same set of genes up- and down-regulated by OCA-B ectopic
512 expression.
513
514 **Fig. 3.** Single-cell RNA-seq analysis of OCA-B-transduced vs. control SMARTA cells at 8 days post
515 LCMV infection. (*A*) UMAP projections of independently clustered EV-transduced (GFP^+) SMARTA
516 cells purified similar to Figs. 2 and 3, and subjected to scRNA-seq. Cluster identities were annotated
517 using a combination of gene expression enrichment (Table S3), cluster identity predictor ImmGen
518 identity scores (Table S4) and PanglaoDB annotation terms. Clusters 1 and 4 were associated with
519 memory formation. Top PanglaoDB annotation terms for cluster 4 are shown below. (*B*) Similar UMAP
520 projection using OCA-B-transduced cells purified from the same mice as in (A). Cluster identities were
521 annotated similarly to (A). Cluster 3 in OCA-B-transduced cells was most strongly associated with
522 memory formation. Top PanglaoDB annotation terms for cluster 3 are shown below.
523 (*C*) Feature plots highlighting expression of representative genes for the two UMAP projections in (A)
524 and (B). (*D*) UMAP projections of the the EV- and OCA-B-transduced single-cell RNA-seq datasets
525 clustered together. For each projection, the percentage of each cluster relative to the total number
526 cells in condition is shown. Cluster identities were annotated using a combination of gene expression
527 enrichment (Table S3), cluster identity predictor ImmGen identity scores (Table S5) and PanglaoDB
528 annotation terms. (*E*) Feature plots highlighting expression of two representative genes (*Tbx21* and
529 *Bcl6*) associated with specific clusters. (*F*) Additional combined feature plots supporting the
530 association of cluster 3 with memory progenitors. (*G*) Violin plots depicting expression of six genes
531 (*Il7r*, *Zeb2*, *Gadd45b*, *Foxo1*, *Tcf7* and *Tox*) across each of the 10 clusters in EV-transduced cells
532 (blue, left) and OCA-B-transduced cells (red, right).
533
534 **Fig. 4.** mCherry expression in splenic T cell populations in specific pathogen-free homozygous OCA-
535 B-3×mCherry mice. (*A*) Mouse *Pou2af1* locus, targeting vector and the targeted *Pou2af1* locus. (*B*)
536 CD4 and CD8 expression are shown for an allelic series of example wild-type (+/+) and homozygous
537 (KI/KI) OCA-B knock-in reporter mice. (*C*) OCA-B homozygous reporter expression in splenic $CD4^+$ T
538 cell populations. (*D*) The same $CD4^+$ cells as in (C) were further stratified by CD62L and CD44 into
539 naïve, early activated, activated and central memory (Tcm) populations. $CD62L^{lo}CD44_{lo}$ cells are likely
540 recently activated cells that have down-regulated CD62L but not yet up-regulated CD44. (*E*) Similar
541 analysis as in (D) except for $CD8^+$ cells.
542
543 **Fig. 5.** $CD4^+$ T cells expressing high levels of OCA-B reporter activity preferentially form central
544 memory cells. (*A*) Schematic for assessing contraction of $mCherry^{hi}$ vs. $mCherry^{lo}$ SMARTA T cells

545 following LCMV infection. Congenically marked SMARTA T cells were isolated from donor mice,
546 transferred into naïve secondary recipients and infected with LCMV. At 8 days post-infection,
547 mCherry^{hi} and mCherry^{lo} populations were isolated by FACS. 8×10^5 SMARTA cells were transferred
548 into naïve recipients. After 8 days, splenic CD4$^+$Ly5.1$^+$5.2$^+$ SMARTA cells were evaluated by flow
549 cytometry. (*B*) Flow cytometric analysis of SMARTA donor T cells engrafted into naïve mice to monitor
550 rates of decline. Representative mice engrafted with mCherry^{lo} (left) or mCherry^{hi} (right) cells are
551 shown. (*C*) Quantification of averaged donor T cell numbers from mice engrafted with mCherry^{lo} or
552 mCherry^{hi} cells. N=7 for the mCherry^{lo} group and N=5 for the mCherry^{hi} group. (*D*) Similar analysis to
553 (C) except quantifying mean mCherry fluorescence intensity. (*E*) Schematic for assessing recall
554 responses of mCherry^{hi} vs. mCherry^{lo} SMARTA T cells following LCMV infection. Congenically
555 marked SMARTA T cells were isolated from donor mice, transferred into naïve secondary recipients
556 and infected with LCMV. However, mice were allowed to clear LCMV and form memory. After 43
557 days, mCherry^{hi} and mCherry^{lo} memory T cell populations were isolated by FACS. 1.3×10^4 SMARTA
558 cells were transferred into naïve recipients, which were infected with LCMV one day later. 7 days
559 post-infection, splenic CD4$^+$Ly5.1$^+$5.2$^+$ SMARTA cells were evaluated by flow cytometry. (*F*) Flow
560 cytometric analysis of SMARTA donor T cells 7 days post-rechallenge to monitor recall responses.
561 Representative mice engrafted with mCherry^{lo} (left) or mCherry^{hi} (right) cells are shown. (*G*)
562 Quantification of averaged donor T cell percentages and numbers from mice engrafted with mCherry^{lo}
563 or mCherry^{hi} cells. N=7 for the mCherry^{lo} group and N=5 for the mCherry^{hi} group. (*H*) Similar analysis
564 to (G) except quantifying mean mCherry fluorescence intensity. (*I*) Schematic for assessing mCherry
565 levels in SMARTA T at early timepoints following LCMV infection. 2×10^5 congenically marked
566 (CD45.1$^+$) SMARTA T cells were isolated from donor mice and transferred into naïve secondary
567 recipients. One day later mice were intraperitoneally infected with 2×10^5 PFU LCMV. Splenic T cells
568 were collected at 3 dpi. (*J*) Gated unfixed splenic CD4$^+$ T cells were assessed for the SMARTA
569 congenic marker Ly5.1 and mCherry (left), while fixed Ly5.1$^+$ (SMARTA) cells from the same mice
570 were used to assess CD25 and TCF1 (right). (*K*) CD25 and mCherry expression were assessed from
571 a representative animal. Left: distribution of SMARTA cell CD25 and mCherry expression in SMARTA
572 mice. Right: CD25 levels of gated mCherry^{hi} and mCherry^{lo} SMARTA cells displayed as a
573 concatenated histogram. (*L*) Quantification of averaged mCherry MFI in CD25^{hi} and CD25^{lo} cells (left),
574 and frequencies (center) and numbers (right) of CD25^{lo} cells in mCherry^{lo} or mCherry^{hi} cells SMARTA
575 T cells. N=6 independent recipient mice.

576 **References and Notes**

577 1. F. Sallusto, A. Lanzavecchia, K. Araki, R. Ahmed, From vaccines to memory and back.
578 *Immunity* **33**, 451-463 (2010).
579 2. S. V. Gearty *et al.*, An autoimmune stem-like CD8 T cell population drives type 1 diabetes.
580 *Nature* **602**, 156-161 (2022).
581 3. A. Schnell *et al.*, Stem-like intestinal Th17 cells give rise to pathogenic effector T cells during
582 autoimmunity. *Cell* **184**, 6281-6298 e6223 (2021).
583 4. P. C. Rosato *et al.*, Virus-specific memory T cells populate tumors and can be repurposed for
584 tumor immunotherapy. *Nat Commun* **10**, 567 (2019).
585 5. G. Cafri *et al.*, Memory T cells targeting oncogenic mutations detected in peripheral blood of
586 epithelial cancer patients. *Nat Commun* **10**, 449 (2019).
587 6. L. A. Shaw *et al.*, Id3 expression identifies CD4(+) memory Th1 cells. *Proc Natl Acad Sci U S*
588 *A* **119**, e2204254119 (2022).
589 7. R. L. Rutishauser *et al.*, Transcriptional repressor Blimp-1 promotes CD8(+) T cell terminal
590 differentiation and represses the acquisition of central memory T cell properties. *Immunity* **31**,
591 296-308 (2009).
592 8. A. Kallies, A. Xin, G. T. Belz, S. L. Nutt, Blimp-1 transcription factor is required for the
593 differentiation of effector CD8(+) T cells and memory responses. *Immunity* **31**, 283-295 (2009).
594 9. H. M. Shin *et al.*, Epigenetic modifications induced by Blimp-1 Regulate CD8(+) T cell memory
595 progression during acute virus infection. *Immunity* **39**, 661-675 (2013).
596 10. L. Pace *et al.*, The epigenetic control of stemness in CD8(+) T cell fate commitment. *Science*
597 **359**, 177-186 (2018).
598 11. H. D. Marshall *et al.*, Differential expression of Ly6C and T-bet distinguish effector and
599 memory Th1 CD4(+) cell properties during viral infection. *Immunity* **35**, 633-646 (2011).
600 12. N. S. Joshi *et al.*, Inflammation directs memory precursor and short-lived effector CD8(+) T cell
601 fates via the graded expression of T-bet transcription factor. *Immunity* **27**, 281-295 (2007).
602 13. R. Hess Michelini, A. L. Doedens, A. W. Goldrath, S. M. Hedrick, Differentiation of CD8
603 memory T cells depends on Foxo1. *J Exp Med* **210**, 1189-1200 (2013).
604 14. R. R. Rao, Q. Li, M. R. Gubbels Bupp, P. A. Shrikant, Transcription factor Foxo1 represses T-
605 bet-mediated effector functions and promotes memory CD8(+) T cell differentiation. *Immunity*
606 **36**, 374-387 (2012).
607 15. M. Pepper, A. J. Pagan, B. Z. Igyarto, J. J. Taylor, M. K. Jenkins, Opposing signals from the
608 Bcl6 transcription factor and the interleukin-2 receptor generate T helper 1 central and effector
609 memory cells. *Immunity* **35**, 583-595 (2011).
610 16. H. Ichii *et al.*, Bcl6 is essential for the generation of long-term memory CD4+ T cells. *Int*
611 *Immunol* **19**, 427-433 (2007).
612 17. A. Banerjee *et al.*, Cutting edge: The transcription factor eomesodermin enables CD8+ T cells
613 to compete for the memory cell niche. *J Immunol* **185**, 4988-4992 (2010).
614 18. D. T. Utzschneider *et al.*, T Cell Factor 1-Expressing Memory-like CD8(+) T Cells Sustain the
615 Immune Response to Chronic Viral Infections. *Immunity* **45**, 415-427 (2016).
616 19. P. Sauter, P. Matthias, The B cell-specific coactivator OBF-1 (OCA-B, Bob-1) is inducible in T
617 cells and its expression is dispensable for IL-2 gene induction. *Immunobiology* **198**, 207-216
618 (1997).
619 20. S. Zwilling, A. Dieckmann, P. Pfisterer, P. Angel, T. Wirth, Inducible expression and
620 phosphorylation of coactivator BOB.1/OBF.1 in T cells. *Science* **277**, 221-225. (1997).
621 21. A. Shakya *et al.*, Oct1 and OCA-B are selectively required for CD4 memory T cell function. *J*
622 *Exp Med* **212**, 2115-2131 (2015).
623 22. J. P. Snook, C. Kim, M. A. Williams, TCR signal strength controls the differentiation of CD4(+)
624 effector and memory T cells. *Sci Immunol* **3**, eaas9103 (2018).
625 23. S. Chevrier, T. Kratina, D. Emslie, A. Karnowski, L. M. Corcoran, Germinal center-
626 independent, IgM-mediated autoimmunity in sanroque mice lacking Obf1. *Immunol Cell Biol*
627 **92**, 12-19 (2014).

24. M. Nakamura *et al.*, Genome-wide association study identifies TNFSF15 and POU2AF1 as susceptibility loci for primary biliary cirrhosis in the Japanese population. *Am J Hum Genet* **91**, 721-728 (2012).
25. M. Ban *et al.*, Linkage disequilibrium screening for multiple sclerosis implicates JAG1 and POU2AF1 as susceptibility genes in Europeans. *J Neuroimmunol* **179**, 108-116 (2006).
26. H. Kim *et al.*, Targeting OCA-B/Pou2af1 blocks activated, autoreactive T cells in the pancreas and type-1 diabetes. *J Exp Med* **218**, e20200533 (2021).
27. H. Shen *et al.*, Recombinant Listeria monocytogenes as a live vaccine vehicle for the induction of protective anti-viral cell-mediated immunity. *Proc Natl Acad Sci U S A* **92**, 3987-3991 (1995).
28. A. Oxenius, M. F. Bachmann, R. M. Zinkernagel, H. Hengartner, Virus-specific MHC-class II-restricted TCR-transgenic mice: effects on humoral and cellular immune responses after viral infection. *Eur J Immunol* **28**, 390-400 (1998).
29. L. Liu *et al.*, Gadd45 beta and Gadd45 gamma are critical for regulating autoimmunity. *J Exp Med* **202**, 1341-1347 (2005).
30. P. Rodriguez-Jimenez *et al.*, Growth arrest and DNA damage-inducible proteins (GADD45) in psoriasis. *Sci Rep* **11**, 14579 (2021).
31. Y. Luo *et al.*, Suppression of collagen-induced arthritis in growth arrest and DNA damage-inducible protein 45beta-deficient mice. *Arthritis Rheum* **63**, 2949-2955 (2011).
32. S. Ju *et al.*, Gadd45b and Gadd45g are important for anti-tumor immune responses. *Eur J Immunol* **39**, 3010-3018 (2009).
33. A. Lachmann *et al.*, ChEA: transcription factor regulation inferred from integrating genome-wide ChIP-X experiments. *Bioinformatics* **26**, 2438-2444 (2010).
34. J. N. Blattman *et al.*, Estimating the precursor frequency of naive antigen-specific CD8 T cells. *J Exp Med* **195**, 657-664 (2002).
35. A. Crawford *et al.*, Molecular and transcriptional basis of CD4(+) T cell dysfunction during chronic infection. *Immunity* **40**, 289-302 (2014).
36. T. Samardzic, D. Marinkovic, P. J. Nielsen, L. Nitschke, T. Wirth, BOB.1/OBF.1 deficiency affects marginal-zone B-cell compartment. *Mol Cell Biol* **22**, 8320-8331 (2002).
37. R. Ahmed, A. Salmi, L. D. Butler, J. M. Chiller, M. B. Oldstone, Selection of genetic variants of lymphocytic choriomeningitis virus in spleens of persistently infected mice. Role in suppression of cytotoxic T lymphocyte response and viral persistence. *J Exp Med* **160**, 521-540 (1984).
38. C. Kim, D. C. Jay, M. A. Williams, Stability and function of secondary Th1 memory cells are dependent on the nature of the secondary stimulus. *J Immunol* **189**, 2348-2355 (2012).
39. D. M. Mitchell, E. V. Ravkov, M. A. Williams, Distinct roles for IL-2 and IL-15 in the differentiation and survival of CD8+ effector and memory T cells. *J Immunol* **184**, 6719-6730 (2010).
40. Y. Luo, R. G. Roeder, Cloning, functional characterization, and mechanism of action of the B-cell-specific transcriptional coactivator OCA-B. *Mol. Cell. Biol.* **15**, 4115-4124 (1995).
41. A. Shakya, J. Kang, J. Chumley, M. A. Williams, D. Tantin, Oct1 is a switchable, bipotential stabilizer of repressed and inducible transcriptional states. *J Biol Chem* **286**, 450-459 (2011).
42. K. Murali-Krishna *et al.*, Counting antigen-specific CD8 T cells: a reevaluation of bystander activation during viral infection. *Immunity* **8**, 177-187 (1998).
43. M. A. Williams, E. V. Ravkov, M. J. Bevan, Rapid culling of the CD4+ T cell repertoire in the transition from effector to memory. *Immunity* **28**, 533-545 (2008).
44. J. Perovanovic *et al.*, Oct1 cooperates with the Smad family of transcription factors to promote mesodermal lineage specification. *Sci. Signal.* **16**, eadd5750 (2023).
45. M. I. Love, W. Huber, S. Anders, Moderated estimation of fold change and dispersion for RNA-seq data with DESeq2. *Genome Biol* **15**, 550 (2014).
46. T. Stuart *et al.*, Comprehensive Integration of Single-Cell Data. *Cell* **177**, 1888-1902 e1821 (2019).

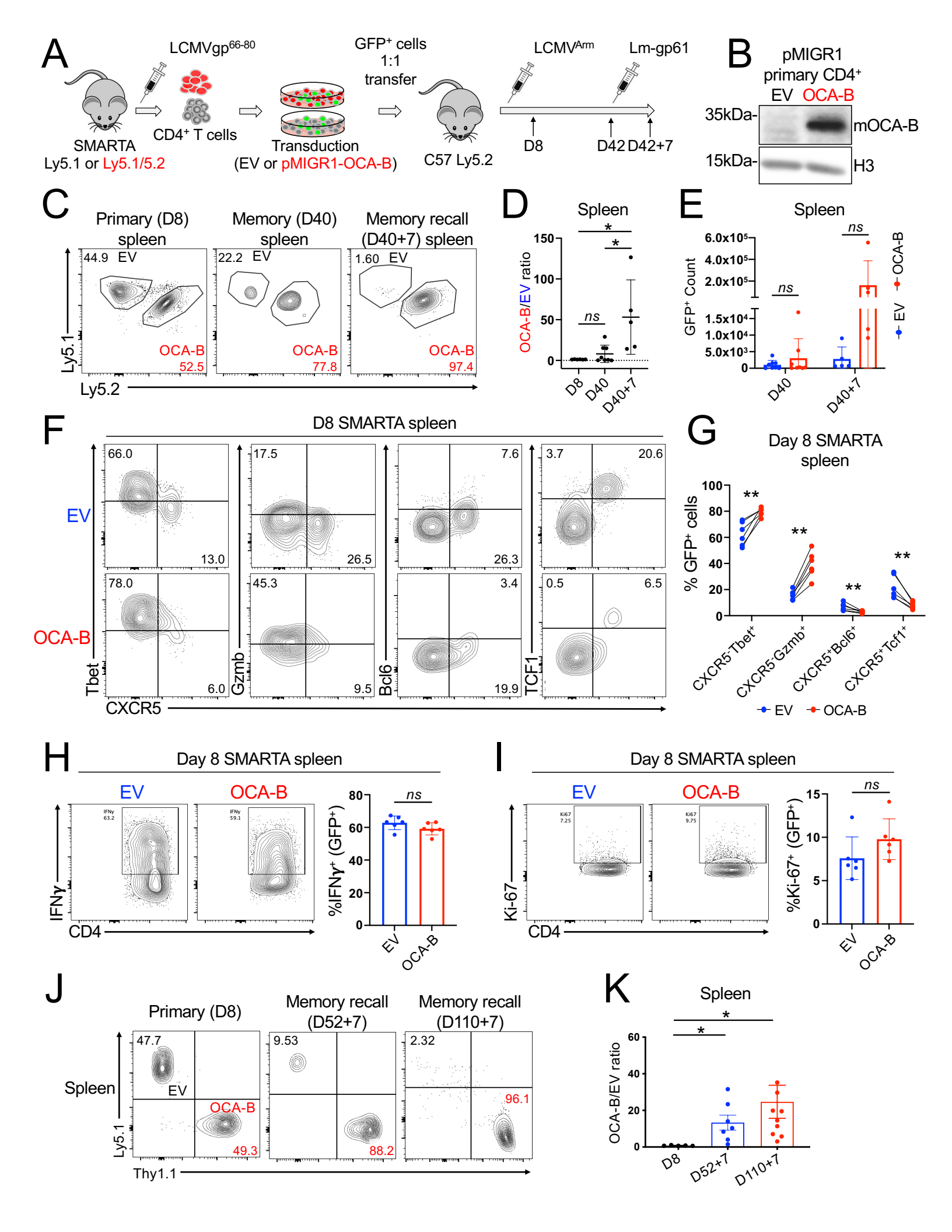
A
LCMVgp66-80
GFP+ cells
1:1
transfer
LCMVArm
Lm-gp61
SMARTA
Ly5.1 or Ly5.1/5.2
CD4+ T cells
Transduction
(EV or pMIGR1-OCA-B)
C57 Ly5.2
D8
D42
D42+7
B
pMIGR1
primary CD4+
EV
OCA-B
35kDa-
mOCA-B
15kDa-
H3
C
Primary (D8)
spleen
Memory (D40)
spleen
Memory recall
(D40+7) spleen
44.9
EV
OCA-B
52.5
22.2
EV
OCA-B
77.8
1.60
EV
OCA-B
97.4
Ly5.1
Ly5.2
D
Spleen
OCA-B/EV ratio
ns
D8
D40
D40+7
E
Spleen
GFP+ Count
ns
OCA-B
EV
D40
D40+7
F
D8 SMARTA spleen
EV
OCA-B
66.0
13.0
17.5
26.5
7.6
26.3
3.7
20.6
78.0
6.0
45.3
9.5
3.4
19.9
0.5
6.5
Tbet
Gzmb
Bcl6
TCF1
CXCR5
G
Day 8 SMARTA
spleen
% GFP+ cells
CXCR5-Tbet+
CXCR5-Gzmb+
CXCR5+Bcl6+
CXCR5+Tcf1+
EV
OCA-B
H
Day 8 SMARTA spleen
EV
OCA-B
IFNγ
CD4
%IFNγ+ (GFP+)
ns
EV
OCA-B
I
Day 8 SMARTA spleen
EV
OCA-B
Ki-67
CD4
%Ki-67+ (GFP+)
ns
EV
OCA-B
J
Primary (D8)
Memory recall
(D52+7)
Memory recall
(D110+7)
Spleen
47.7
EV
OCA-B
49.3
9.53
88.2
2.32
96.1
Ly5.1
Thy1.1
K
Spleen
OCA-B/EV ratio
D8
D52+7
D110+7

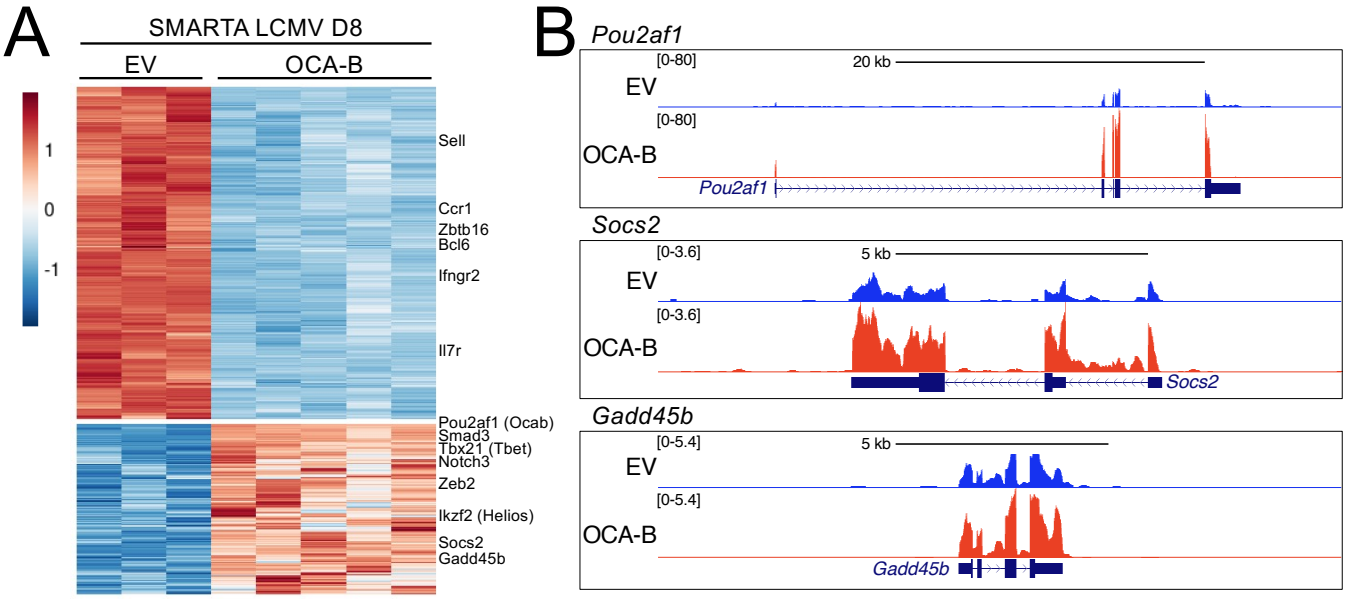

C

OCA-B upregulated genes

Epigenomic roadmap HM	*p*-value
H3K9me3 Breast vHMEC	0.048
Molecular function	***p*-value**
Toll-like receptor binding	0.006
Aspartic-type peptidase activity	0.007

OCA-B downregulated genes

Epigenomic roadmap HM	*p*-value
H3K27me3 CD4 Memory Primary Cells	1.45E-04
H3K27me3 CD8 Memory Primary Cells	9.30E-04
Molecular function	***p*-value**
Superoxide-generating NADPH oxidase activator activity	1.29E-09
Cytokine receptor activity	1.24E-06

D

OCA-B upregulated genes

ChEA 2016	*p*-value
Tp53	0.01936
Smc3	0.02544

OCA-B downregulated genes

ChEA 2016	*p*-value
IRF8	1.24E-20
SMRT	1.14E-15
MYB	1.73E-09
Nerf2	4.79E-09
NCOR	1.52E-08

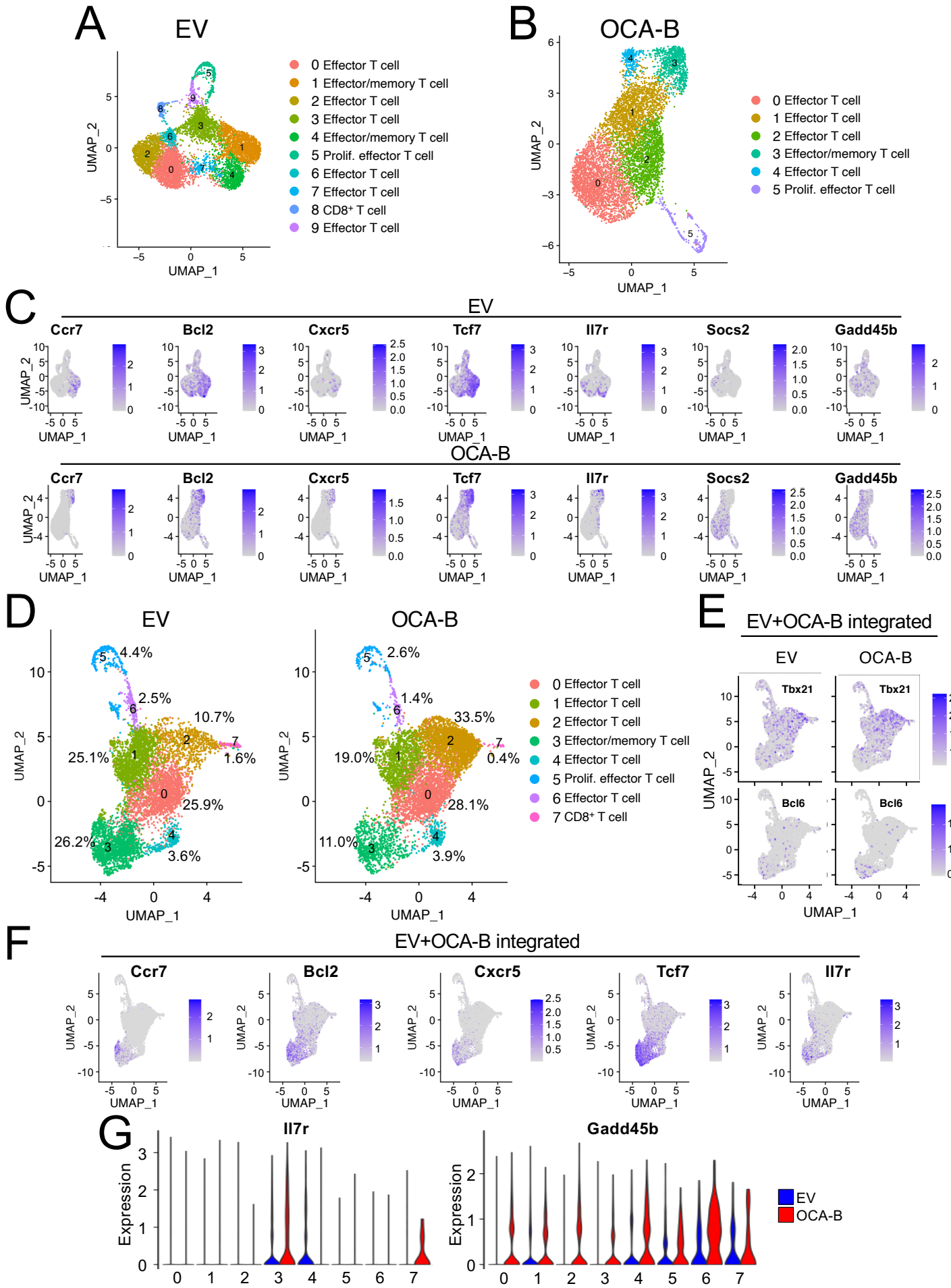
A
EV
0 Effector T cell
1 Effector/memory T cell
2 Effector T cell
3 Effector T cell
4 Effector/memory T cell
5 Prolif. effector T cell
6 Effector T cell
7 Effector T cell
8 CD8+ T cell
9 Effector T cell
UMAP_1
UMAP_2
B
OCA-B
0 Effector T cell
1 Effector T cell
2 Effector T cell
3 Effector/memory T cell
4 Effector T cell
5 Prolif. effector T cell
C
EV
Ccr7
Bcl2
Cxcr5
Tcf7
Il7r
Socs2
Gadd45b
OCA-B
D
EV
OCA-B
4.4%
2.5%
10.7%
1.6%
25.1%
25.9%
26.2%
3.6%
2.6%
1.4%
33.5%
0.4%
19.0%
28.1%
11.0%
3.9%
0 Effector T cell
1 Effector T cell
2 Effector T cell
3 Effector/memory T cell
4 Effector T cell
5 Prolif. effector T cell
6 Effector T cell
7 CD8+ T cell
E
EV+OCA-B integrated
EV
OCA-B
Tbx21
Bcl6
F
EV+OCA-B integrated
Ccr7
Bcl2
Cxcr5
Tcf7
Il7r
G
Il7r
Gadd45b
Expression
EV
OCA-B

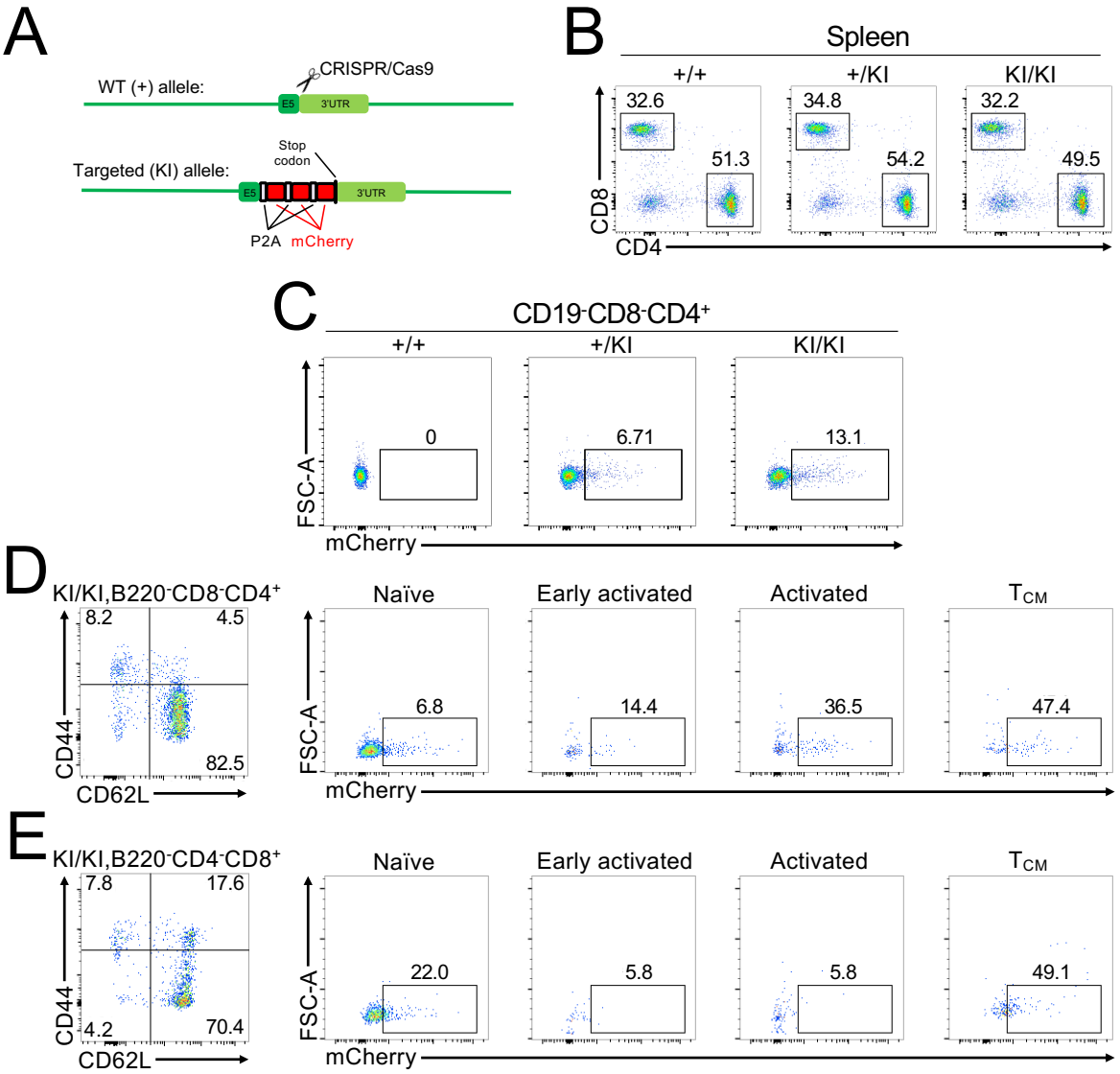
A
WT (+) allele:
CRISPR/Cas9
E5
3'UTR
Targeted (KI) allele:
Stop codon
P2A
mCherry
B
Spleen
+/+
+/KI
KI/KI
32.6
51.3
34.8
54.2
32.2
49.5
CD8
CD4
C
CD19-CD8-CD4+
+/+
+/KI
KI/KI
0
6.71
13.1
FSC-A
mCherry
D
KI/KI,B220-CD8-CD4+
8.2
4.5
82.5
CD44
CD62L
Naïve
Early activated
Activated
TCM
6.8
14.4
36.5
47.4
FSC-A
mCherry
E
KI/KI,B220-CD4-CD8+
7.8
17.6
4.2
70.4
CD44
CD62L
Naïve
Early activated
Activated
TCM
22.0
5.8
5.8
49.1
FSC-A
mCherry

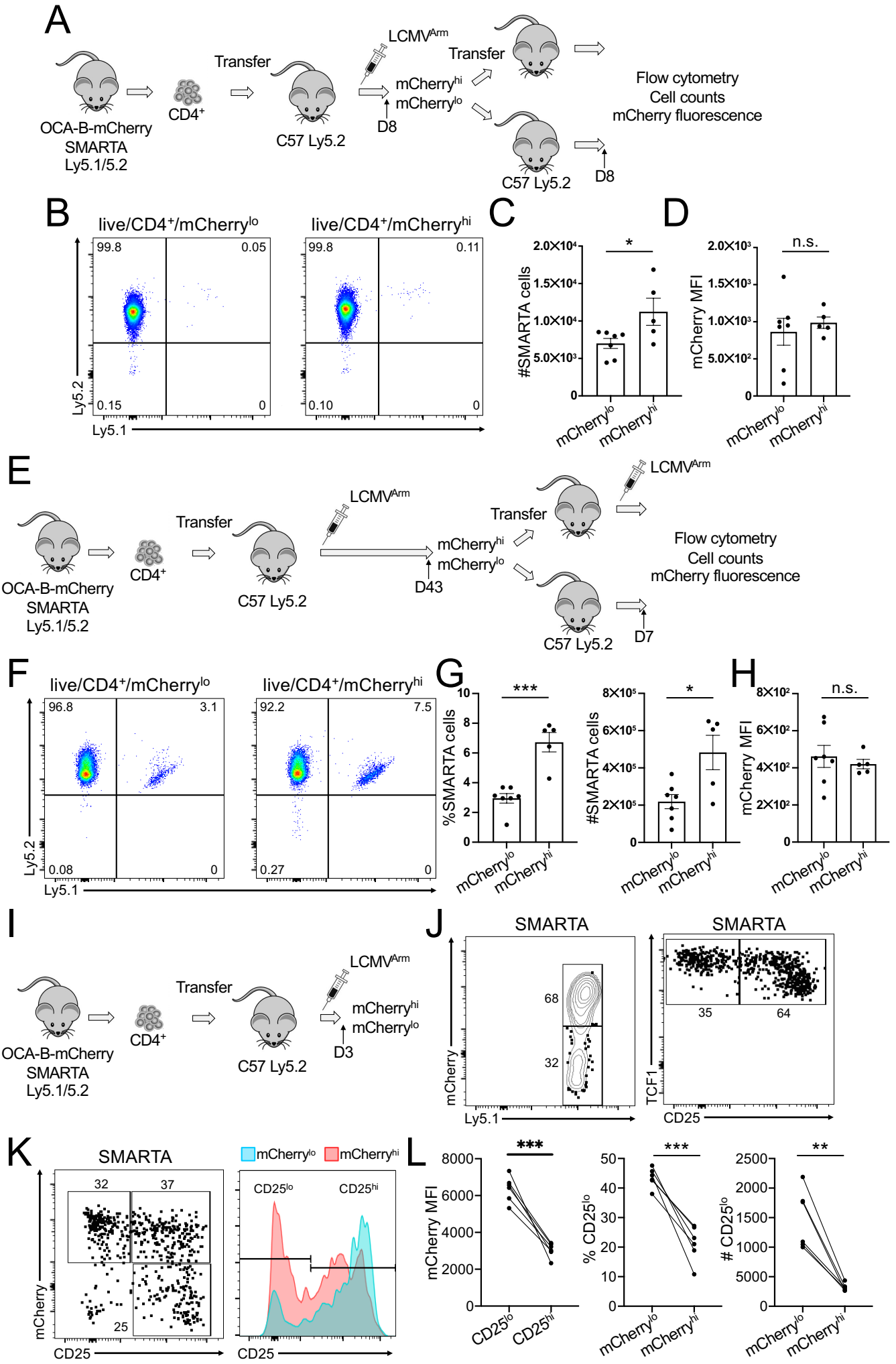
A
OCA-B-mCherry
SMARTA
Ly5.1/5.2
CD4+
Transfer
C57 Ly5.2
LCMVArm
D8
mCherryhi
mCherrylo
Transfer
C57 Ly5.2
D8
Flow cytometry
Cell counts
mCherry fluorescence
B
live/CD4+/mCherrylo
live/CD4+/mCherryhi
99.8
0.05
0.15
0
99.8
0.11
0.10
0
Ly5.2
Ly5.1
C
#SMARTA cells
2.0X10⁴
1.5X10⁴
1.0X10⁴
5.0X10³
0
*
mCherrylo
mCherryhi
D
mCherry MFI
2.0X10³
1.5X10³
1.0X10³
5.0X10²
0
n.s.
mCherrylo
mCherryhi
E
OCA-B-mCherry
SMARTA
Ly5.1/5.2
CD4+
Transfer
C57 Ly5.2
LCMVArm
D43
mCherryhi
mCherrylo
Transfer
LCMVArm
C57 Ly5.2
D7
Flow cytometry
Cell counts
mCherry fluorescence
F
live/CD4+/mCherrylo
live/CD4+/mCherryhi
96.8
3.1
0.08
0
92.2
7.5
0.27
0
Ly5.2
Ly5.1
G
%SMARTA cells
10
8
6
4
2
0
***
mCherrylo
mCherryhi
#SMARTA cells
8X10⁵
6X10⁵
4X10⁵
2X10⁵
0
*
mCherrylo
mCherryhi
H
mCherry MFI
8X10²
6X10²
4X10²
2X10²
0
n.s.
mCherrylo
mCherryhi
I
OCA-B-mCherry
SMARTA
Ly5.1/5.2
CD4+
Transfer
C57 Ly5.2
LCMVArm
D3
mCherryhi
mCherrylo
J
SMARTA
68
32
mCherry
Ly5.1
SMARTA
35
64
TCF1
CD25
K
SMARTA
32
37
25
mCherry
CD25
mCherrylo
mCherryhi
CD25lo
CD25hi
CD25
L
mCherry MFI
8000
6000
4000
2000
0
***
CD25lo
CD25hi
% CD25lo
50
40
30
20
10
0
***
mCherrylo
mCherryhi
CD25lo
2500
2000
1500
1000
5000
0
**
mCherrylo
mCherryhi